Foxn3 is part of a transcriptional network that regulates cilia genes in the developing mouse retina

Huanqing Zhang[1], Fan Meng[1,2], and David L. Turner[1,3*]

1) Michigan Neuroscience Institute, University of Michigan, Ann Arbor, MI 48109

2) Department of Psychiatry, University of Michigan, Ann Arbor, MI 48109

3) Department of Biological Chemistry, University of Michigan, Ann Arbor, MI 48109

*author for correspondence: David L. Turner, dlturner@umich.edu

Abstract

The forkhead transcription factor Foxn3 is a transcriptional repressor. Analysis of embryonic retinas from mice with a targeted disruption of the Foxn3 gene revealed upregulation of numerous genes linked to cilia structure or assembly. Foxj1, a forkhead transcription factor required for motile cilia, was upregulated, along with multiple target genes of Foxj1. Primary cilia in the developing retina showed structural changes in the absence of Foxn3. CUT&RUN analysis revealed that many of the upregulated genes were bound by the Foxn3 protein and also by the Rfx3 transcription factor. The Foxn3 protein forms a complex with the Rfx3 protein, and a short protein motif shared by Foxj1, Foxn4, and Foxn3 is required for complex formation with Rfx3. The same shared motif is required for transcriptional repression by Foxn3, as well as for full transcriptional activation by Foxn4 with Rfx3. These results reveal a new layer of transcriptional regulation of genes required for cilia and show that Foxn3 prevents inappropriate expression of cilia genes in the developing retina.

Introduction

Cilia are thin, filamentous, membrane-enclosed structures with a microtubule core, present on cells in many eukaryotes (reviewed in Derderian et al., 2023). Motile cilia can direct fluid flow or drive cellular movement, while primary cilia (also known as sensory cilia) mediate reception of extracellular signals that include Sonic Hedgehog (SHH), TGFβ, Wnt, and Notch. In the retina, photoreceptor outer segments are specialized primary cilia used for phototransduction, while retinal ganglion cells, amacrine interneurons, and Müller glia have been reported to have primary cilia in the mouse (Chen et al., 2021; Kowal et al., 2022; Ning et al., 2021). During development, retinal progenitor cells have primary cilia located at the outer surface of the retina (Burnett et al., 2017; Dubaic et al., 2023). The assembly and function of cilia involves proteins produced by hundreds of different genes; ciliopathies can arise from mutations in many of these genes. Ciliopathies frequently affect photoreceptors, lead to retinal degeneration, and impact vision (Chen et al., 2021). Defects in primary cilia or signaling pathways in primary cilia can alter cell fates or retinal structure during development (Cwinn et al., 2011; Dilan et al., 2019; Fiore et al., 2020; Wang et al., 2005; Zhang and Yang, 2001).

Members of the forkhead and RFX transcription factor protein families have been found to regulate genes associated with cilia in multiple organisms. Forkhead proteins are an ancient family of eukaryotic transcription factors that bind DNA via the forkhead domain and have multiple roles in development (reviewed in Herman et al., 2021). In vertebrates, the forkhead protein Foxj1 regulates genes encoding components of motile cilia (Choksi et al., 2014; Patir et al., 2020; Vij et al., 2012; Yu et al., 2008). Foxj1 cooperates with the Rfx2-3

transcription factors to regulate genes involved in motile cilia (Didon et al., 2013; Lemeille et al., 2020). Foxn4 functions with Foxj1 to allow the generation of multicileated cells (Campbell et al., 2016; Quigley and Kintner, 2017). A Foxj1 homolog is necessary for neurogenesis during zebrafish retinal regeneration after injury, although Foxj1 is not required for retinal development in zebrafish (Lyu et al., 2023).

Over 40 genes encode forkhead proteins in mice or humans, and mutations in forkhead genes are associated with genetic diseases in both organisms (Herman et al., 2021). The Foxn subfamily of forkhead proteins has four members in mice and humans. Foxn1 is mutated in nude mice and is required for T-cell development in both mice and humans (Boehm et al., 2003; Žuklys et al., 2016). Foxn4 is expressed in a subset of retinal precursor cells and is required for the formation of most or all horizontal and many amacrine interneurons in the retina (Li et al., 2004). Foxn4 plays an essential role in developmental timing in the retina, promoting interneuron and photoreceptor formation while suppressing retinal ganglion cells (Liu et al., 2020). Foxn4 also functions in spinal cord interneuron development (Misra et al., 2014), and has been linked to heart development in zebrafish (Chi et al., 2008). Foxn1 and Foxn4 share sequence similarity outside of the forkhead domain, and Foxn4 can partially substitute for Foxn1 in mice (Swann et al., 2014). A partial clone of human Foxn3 was originally identified as a DNA damage checkpoint suppressor in a functional screen in yeast, while the full length protein functions as a transcriptional repressor in mammalian cells (Huot et al., 2014; Pati et al., 1997; Scott and Plon, 2005). Foxn3 has been implicated in the regulation of glucose metabolism in liver (Karanth et al., 2019), as well as in the regulation of inflammation in

lungs (Zhu et al., 2023). The Foxn2 protein has extensive sequence similarity to Foxn3, and both proteins have been reported to function as tumor suppressors (reviewed in Song et al., 2023). Most forkhead factors recognize one of two unrelated DNA motifs, depending on their subfamily, but Foxn3 can recognize both types of motifs, potentially allowing it to regulate a larger set of target genes than other forkhead factors (Nakagawa et al., 2013; Rogers et al., 2019).

We identified the Foxn3 mRNA as a target of microRNA miR-216b in the mouse retina (Zhang et al., 2022). Foxn3 is expressed in retinal progenitor cells as well as differentiated bipolar and cholinergic amacrine cells (Boudreau-Pinsonneault et al., 2023; Zhang et al., 2022). When overexpressed in the neonatal retina, miR-216b promotes the generation of additional amacrine cells and the loss of bipolar cells. Co-expression of Foxn3 partially reversed this effect, while inhibition of Foxn3 generated similar phenotypes (Zhang et al., 2022). To further investigate the role of Foxn3 in the developing retina, we analyzed retinas from embryonic mice in which both copies of the Foxn3 gene are disrupted (Birling et al., 2021). We did not observe an obvious change in the number of amacrine cells generated in the developing retinas from Foxn3-/- mice. However, in embryonic retinas without functional Foxn3, numerous genes involved in cilia formation and function were upregulated, and primary cilia on retinal progenitor cells were altered. We identified genomic regions bound by Foxn3, as well as by Foxn4 and by Rfx3, in the developing retina. Most Foxn3 binding regions overlap with regions bound by Rfx3. We show that Foxn3 forms a complex with Rfx3. We find that the Foxn3, Foxn4, and Foxj1 proteins share an amino acid motif that is required for complex formation with Rfx3, as well

as for cooperative transcriptional activation or repression by Rfx3 with Foxn4 or Foxn3 respectively. Our results indicate that Foxn3 is an important negative regulator of cilia genes in the retina. In other tissues Foxn4 and Foxj1 direct the formation of multiple motile cilia. We propose that Foxn3 may prevent Foxn4 from inappropriately upregulating Foxj1 and other genes involved in motile cilia formation in the retina.

Results

Genes associated with cilia are upregulated in Foxn3-/- retinas

Mice heterozygous for a targeted deletion of the Foxn3 exon 3 (Birling et al., 2021) were backcrossed. No Foxn3-/- live offspring were observed, consistent with prior reports (Birling et al., 2021; Zhu et al., 2023). However, Foxn3-/- embryos are present at the end of gestation on embryonic day 19 (E19) and appear grossly normal (Birling et al., 2021), indicating that Foxn3 null mice likely die at or shortly after birth. Retina sections from E19 Foxn3-/- embryos did not show obvious changes in amacrine cells or overall retinal structure (Fig.1A-D). We used RNAseq to compare gene expression in retinas isolated from Foxn3+/+ and Foxn3-/- embryos at E19 (Supplemental Table 1). mRNAs specific to various retinal cell types present at E19 did not change significantly in retinas without Foxn3 (Supplemental Table 2), suggesting that overall retina development is not disrupted. However, 930 genes were differentially expressed ($q \leq 0.0001$). Most differentially expressed genes were upregulated in the Foxn3-/- retinas, including nearly all mRNAs that changed more than two-fold (Fig. 1E), consistent with Foxn3 repressing transcription. Foxj1, a transcriptional activator that regulates the gene expression program of motile cilia was upregulated ~20-fold. mRNAs for Rfx1, Rfx2, and Rfx3, three transcription factors linked to cilia gene expression were significantly upregulated in Foxn3-/- retinas, although each increased less than two-fold (Supplemental Table 1). The Foxn3 gene in which exon 3 was deleted expressed an mRNA that spliced exon 2 to exon 4, and that mRNA also was significantly upregulated in Foxn3-/- retinas, although with a less than two-fold increase. Strikingly, the most enriched GO categories for the differentially expressed genes were

components of cilia and/or were associated with cilia assembly (Fig. 1F). Cilia-related GO categories combined included 236 genes, about 25% of all differentially expressed genes. Several genes previously reported to be repressed by Foxn3 overexpression in human cells (Huot et al., 2014) were among the genes upregulated in the retina (e.g., the Pim2 serine/threonine kinase, Dryk3 kinase, Iqck, and Ift88; Supplemental Table 1).

Many retinal progenitor cells have primary cilia located at the outer surface of the retina during retinal development (Burnett et al., 2017; Ning et al., 2021). We examined primary cilia in the retinas from Foxn3-/- and wild-type mice at E19. Immunofluorescence analysis of Arl13b and Ift88, two proteins present in primary cilia, revealed disorganization and structural variability for the primary cilia of Foxn3-/- retinas at E19, when compared to Foxn3+/+ retinas (Fig. 2). The localization and levels of Ift88, a component of intraflagellar transport, varied between cilia in the Foxn3-/- retinas, with more apparent co-localization for Ift88 and Arl13b within the primary cilia than in wild-type retinas.

Identification of genomic binding sites for Foxn3, Rfx3, and Foxn4 in the developing retina

To determine whether genes differentially expressed in Foxn3-/- retinas were likely to be direct targets of Foxn3, we performed CUT&RUN analysis (Skene and Henikoff, 2017) to identify genomic regions bound by Foxn3 in wild-type mouse retinas at E16. 2794 regions with Foxn3 binding were identified (Supplemental Table 3), based on peaks of read enrichment ($q<0.0001$) that were consistent between two separate experiments, each with two anti-Foxn3 samples and two IgG controls. Heat maps for individual CUT&RUN libraries showed consistent signals at the identified Foxn3 binding regions (Fig. 3A). 90% of the

genomic regions bound by Foxn3 overlap with candidate mouse cis-Regulatory Elements (cCREs) annotated by ENCODE (Abascal et al., 2020), with binding at promoters being most frequent (Fig. 3B). We annotated Foxn3-bound regions based on genes with the nearest transcription start site (TSS). 48% of the differentially expressed genes in Foxn3-/- retinas were linked to at least one region bound by Foxn3 in the CUT&RUN analysis, indicating that these genes are likely to be direct targets of Foxn3 regulation (Fig 3C). One example is Foxj1, which had a prominent Foxn3 binding peak at its promoter (Fig 3D). The Foxn3 protein has been shown to bind preferentially to two different, unrelated DNA sequence motifs, referred to as FHL-N, and FKH (Nakagawa et al., 2013; Rogers et al., 2019). The FHL-N motif is a subset of the more degenerate FHL binding motif, which is bound by multiple members of the Forkhead family (Nakagawa et al., 2013). FHL-N, FHL, and FKH motifs were all significantly enriched in Foxn3 binding regions (Fig. 3E). Intriguingly, the most enriched de novo motif in the Foxn3 binding regions was similar to motifs bound by RFX family transcription factors, which are linked to cilia gene regulation (Choksi et al., 2014). Motifs for both Rfx3 (a dimeric RFX binding motif) and Rfx7 (a monomeric RFX binding motif) were enriched in regions bound by Foxn3 (Fig. 3E). Prominent Foxn3 binding peaks are present in the promoters of Tekt1, Ccdc39, and Cfap206 (Fig. 4A), three genes involved in cilia formation that are upregulated in Foxn3-/- retinas (Fig. 1E). We constructed Luciferase reporters driven by the promoter region from each gene and co-transfected the reporters in combination with expression vectors for Foxj1, Rfx3, and/or Foxn3 into HEK293 cells (Fig.4B-D). Foxj1 activated all three reporters ~8-15 fold. We also tested whether the Rfx3 protein could either activate the reporters or

cooperate with Foxj1. Rfx3 by itself activated the reporters less than two-fold, but modestly increased Tekt1 activation when co-expressed with Foxj1. Co-expression of Foxn3 blocked activation of all three reporters by Foxj1, with or without Rfx3, consistent with Foxn3 directly repressing these genes.

To investigate whether Foxn3 genomic binding overlaps with genomic binding for the Rfx3 or Foxn4 proteins in the retina, we used CUT&RUN to identify regions bound by Rfx3 or Foxn4 in wild-type E16 mouse retinas (Fig, 5A-B)(Supplemental Tables 4, 5). Individual CUT&RUN samples showed consistent enrichment at the called peaks (Supplemental Fig. S1). Remarkably, 81% of the Foxn3 binding regions overlapped with regions bound by Rfx3, while 40% of the Foxn3 binding regions overlapped with regions bound by Foxn4; 32% of the Foxn3 binding regions overlapped with both Foxn4 and Rfx3 bound regions (Fig.5C). For Foxn4, 36% of the bound regions overlapped with Rfx3 bound regions. Rfx3 and Rfx7 binding motifs were significantly enriched in the regions bound by Rfx3, while FHL-N and FHL binding motifs were significantly enriched in the Foxn4 bound regions (Fig.5D).

The Foxj1 promoter region was bound by both Foxn3 and Rfx3 in the embryonic retinas, but not by Foxn4 (Fig. 5E). We constructed a Luciferase reporter with the Foxj1promoter region and co-transfected it with expression vectors for Foxn4, Rfx3, and/or Foxn3 into HEK293 cells (Fig. 5F). Rfx3 weakly activated the promoter, while Foxn4 activated the Foxj1 promoter reporter more than 10-fold, and co-expression of Rfx3 with Foxn4 further increased activation. However, co-expression of Foxn3 strongly inhibited activation of the reporter by Foxn4, with or without Rfx3. The Ptprf mRNA was upregulated in Foxn3-/- retinas, and an enhancer located in the intron of Ptprf was bound by Foxn3 and

Rfx3, but not Foxn4, in the retina. A Ptprf reporter was activated by expression of Foxn4 or Rfx3 in HEK293 cells, and further activated by co-expression of Foxn4 and Rfx3 together, while Foxn3 effectively repressed reporter activation (Fig. 6A). We also constructed Luciferase reporters for enhancers located in introns of the Meis1 and Notch1 genes, both of which were by bound by Foxn3, Rfx3, and Foxn4 in the retina, based on our CUT&RUN data. The Meis1 and Notch1 genes have been linked to the Foxn4 pathway in retina and/or spinal cord (Islam et al., 2013; Luo et al., 2012; Misra et al., 2014), and both the Meis1 and Notch1 reporters were activated by co-expression of Foxn4 in HEK293 cells. Activation of the Meis1 reporter by Foxn4 further increased with co-expression of Rfx3, but neither reporter was repressed by co-expression of Foxn3 (Fig. 6B, C). Neither Meis1 nor Notch1 mRNA were upregulated in Foxn3-/- retinas (Supplemental Table 1).

Luciferase reporters based on two intronic enhancers located in the Foxn3 gene that were bound by Foxn3, Rfx3, and Foxn4 were constructed and assayed in HEK293 cells (Fig. 6D-F). Ascl1 is a basic-helix-loop-helix (bHLH) transcription factor that has previously been shown to cooperatively activate transcription with Foxn4 in the retina (Luo et al., 2012). Both reporters were activated by Foxn4, and strongly activated by the combination of Foxn4 with Ascl1 in HEK293 cells (Fig. 6D, F). Co-expression of Rfx3 with either Foxn4 or Foxn4 and Ascl1 together further increased activation of the reporters, while co-expression of Foxn3 strongly inhibited reporter activity driven by Foxn4, Ascl1, or Rfx3, alone or in combination (Fig. 6D, F). For the Foxn3 Enhancer 2 reporter, we tested whether binding sites for each of these factors (Fig. 6E) were required for reporter function. Mutating the two E-boxes (bHLH binding motifs) present in the reporter prevented Ascl1 cooperation with

Foxn4 and Rfx3 (Fig. 6G). Mutation of the FKH and the FHL-N forkhead motifs together in the Foxn3 Enhancer 2 reporter greatly reduced activation by Foxn4 or by Rfx3 with Foxn4 (Fig. 6H). However, activation by Foxn4 still was strongly inhibited by co-expression of Foxn3 with either the reporter with E-box mutations or the reporter with FKH/FHL-N mutations (Fig. 6G, H). Mutation of the single Rfx3 binding motif present in the Foxn3 enhancer 2 reporter greatly reduced activation by Foxn4 with Ascl1 (Fig. 6I). Furthermore, co-expression of Foxn3 failed to inhibit the reporter without the Rfx3 site when activated by Foxn4 with Ascl1 (Fig. 6I). Taken together, these observations suggest that Rfx3 can cooperate with Foxn4 for transcriptional activation, and also can cooperate with Foxn3 for transcriptional repression.

A protein motif in Foxn4, Foxj1, and Foxn3 required for interaction with Rfx3

The mouse Foxn4 and Foxj1 proteins can functionally substitute for the C. elegans FKH-8 protein to support expression of ciliome gene expression in C. elegans (Brocal-Ruiz et al., 2023), and FKH-8 is known to cooperate with DAF-19, the only RFX protein present in C. elegans, to activate cilia gene expression. The Foxj1 protein cooperates with RFX proteins in regulating genes involved in motile cilia formation in mammals, and human Foxj1 and Rfx3 co-immunoprecipitate, showing that these proteins can form a complex (Didon et al., 2013). Large-scale screens for protein-protein interactions have reported association of Foxj1, Foxj2, Foxn2, Foxn3 and Foxn4 with Rfx1, Rfx2, and/or Rfx3 (Huttlin et al., 2021; Huttlin et al., 2017; Li et al., 2015). We looked for amino acid sequences outside of the forkhead domain that were conserved between FKH-8, Foxj1, and

Foxn2/Foxn3/Foxn4 to identify candidate motifs that might mediate complex formation with RFX proteins. A leucine rich LXXLXWL motif is located N-terminal to the forkhead DNA binding region in these proteins (Fig. 7A). A similar sequence with the central leucine substituted by isoleucine or methionine is present in Foxj2 and Foxj3. A divergent motif without the central hydrophobic residue or the conserved tryptophan is present in Foxi1, which fails to substitute for FKH-8 in C. elegans (Brocal-Ruiz et al., 2023). We constructed expression vectors for Foxn4, Foxn3, and Foxj1 in which the LXXLXWL sequence was replaced with seven alanine residues (Foxn4-7A, Foxn3-7A, and Foxj1-7A, Fig. 7A). Hemagglutinin- (HA-) epitope-tagged versions of Foxn4, Foxn3, and Foxj1 proteins co-immunoprecipitated with Rfx3 when the co-expressed in HEK293 cells, but HA-epitope-tagged versions of the Foxn4-7A, Foxn3-7A, and Foxj1-7A proteins showed no co-immunoprecipitation with Rfx3 (Fig. 7B). A Foxn4-7A expression vector failed to activate the Foxn3 enhancer 2 reporter and showed reduced activation when combined with Rfx3, while a Foxn3-7A expression vector could not inhibit activation of the same reporter by Foxn4 and Ascl1 (Fig. 7C). Together with previous reports, these observations indicate that the Rfx3 protein forms a complex with Foxn3, Foxn4, or Foxj1 to promote transcriptional regulation of target genes, and that all three forkhead proteins require the conserved LXXLXWL motif for complex formation with Rfx3.

Foxn3-/- mice, which have Foxn3 exon 3 deleted, express a Foxn3 mRNA in which exon 2 splices to exon 4. The N-terminus of Foxn3, including the LXXLXWL motif and part of the forkhead domain are present in exon 2. The C-terminus of Foxn3, encoded by exons 4 and 5, is out of frame when exon 2 splices to exon 4, potentially creating a truncated Foxn3

protein with a novel C-terminus. To test whether the truncated and altered Foxn3 protein was functional, we constructed an expression vector for Foxn3 without exon 3. Co-expression of the truncated Foxn3 protein had no effect on the activation of the Foxn3 Enhancer 2 reporter by Foxn4, Ascl1, and Rfx3, suggesting that the truncated Foxn3 protein in the Foxn3-/- mice is not functional (Supplemental Fig. S2).

Discussion

Over 200 genes involved in cilia formation or function were upregulated in the developing retinas of mice with a targeted disruption of the Foxn3 gene. The levels of the most highly upregulated retinal mRNAs increased over 100-fold. CUT&RUN analysis revealed that about half of Foxn3 regulated genes in the retina were bound by the Foxn3 protein, consistent with direct repression of these genes by Foxn3 (Scott and Plon, 2005). Our results are also consistent with the observation that overexpression of Foxn3 in human lung carcinoma cells downregulated multiple genes involved in cilium biogenesis, as well as other genes, and reduced the formation of primary cilia on the cultured cells (Huot et al., 2014). The promoter of Foxj1, a transcriptional activator previously linked to cilia gene expression, was highly bound by Foxn3 and the Foxj1 mRNA was upregulated more than 20-fold in the Foxn3-/- retinas. Reporters based on the promoters from Tekt1, Ccdc39, and Cfap206, three cilia-linked genes upregulated in the absence of Foxn3, were activated by Foxj1, consistent with previous reports that these three genes are regulated by Foxj1 (Beckers et al., 2020; Didon et al., 2013; Stauber et al., 2017). Foxj1 activation of the three reporters was repressed by co-expression of Foxn3, indicating that Foxn3 can repress targets of Foxj1. These observations suggest that the loss of Foxn3 derepresses the Foxj1 gene as well as other genes; subsequent Foxj1 protein expression likely further activates some derepressed Foxn3 targets.

Forkhead proteins and the RFX transcription factors have been linked to the activation of cilia gene expression in both vertebrates and invertebrates. In vertebrates, Foxj1 is required for expression of genes required for motile cilia (Choksi et al., 2014; Patir

et al., 2020; Stauber et al., 2017; Yu et al., 2008), while Foxn4 cooperates with Foxj1 to generate multicileated cells (Campbell et al., 2016). The Rfx1-4 proteins have been linked to both primary and motile cilia, with both redundant and specific roles for individual family members (Lemeille et al., 2020; Sugiaman-Trapman et al., 2018). Foxj1 can cooperate with RFX proteins, and can co-immunoprecipitate with Rfx3 (Didon et al., 2013), while interactions between RFX proteins and Foxj1, Foxn4, Foxn2, and Foxn3 have been reported (Huttlin et al., 2021; Huttlin et al., 2017; Li et al., 2015). The nematode C. elegans, which has sensory cilia but lacks motile cilia, has one Forkhead homolog, FKH-8, and one RFX homolog, DAF-19, which synergistically activate cilia gene expression; either mouse Foxj1 or mouse Foxn4 can substitute for FKH-8 in C. elegans (Brocal-Ruiz et al., 2023). Here we found that Rfx3 genomic binding in the embryonic mouse retina extensively overlaps with Foxn3 binding, and overlaps to a lesser extent with Foxn4 binding. Reporters based on genomic regulatory elements bound by these proteins could be cooperatively activated by Foxn4 and Rfx3 in cell culture, but were repressed by Foxn3. We found that a conserved LXXLXWL motif is present in FKH-8 and the mouse Foxj1, Foxn4, Foxn2, and Foxn3 proteins. Substitution of the LXXLXWL motif with alanines prevented association between Rfx3 and the Foxj1, Foxn4, and Foxn3 proteins, reduced cooperative activation of a reporter by Foxn4 with Rfx3, and prevented Foxn3 reporter repression. While Rfx3 by itself had modest effects on reporter expression, mutation of the Rfx3 binding site in Foxn3 enhancer 2 reporter reduced cooperative activation by Foxn4 and prevented repression by Foxn3. Based on these observations, cooperation between Foxn4 or Foxj1 and Rfx3 likely involves both binding to nearby genomic sites and the formation of protein-protein complexes. The Foxn3

protein includes transcriptional repression domains located C-terminal to the forkhead domain (Huot et al., 2014; Scott and Plon, 2005). Foxn3 binds to similar DNA sequences as Foxn4, although Foxn3 can bind to additional DNA sequences as well (Nakagawa et al., 2013; Rogers et al., 2019). This suggests that Foxn3 could repress by competing with Foxn4 for DNA binding sites, as well as by recruiting transcriptional corepressors. Since Foxn3 and Foxn4 both require the LXXLXWL motif for complex formation with Rfx3, Foxn3 may further compete with Foxn4 for protein interactions. Such multifaceted competition could allow more potent repression by Foxn3.

RFX proteins have been associated with both activation and repression of target genes (Didon et al., 2013; Iwama et al., 1999; Nakayama et al., 2003). The extensive overlap between Rfx3 and Foxn3 genomic binding in the developing retina raises the possibility that Foxn3 represses numerous genes in part by interaction with Rfx3. Some of the shared binding sites for Foxn3 and Rfx3 detected by CUT&RUN contain one or more RFX binding motifs but do not contain an apparent Foxn3 binding motif (e.g., the Ptprf intronic enhancer in Fig. 6A). These observations suggest that Foxn3 may be recruited into complexes with DNA-bound Rfx3 without direct DNA binding by Foxn3. Alternately, Foxn3 in a complex with Rfx3 may be able to bind to a non-canonical DNA binding site, as reported for cooperative binding by other transcription factors (Berkes et al., 2004). Genetic disruptions of Rfx3 or other RFX factors are associated with human neurodevelopmental disorders (Harris et al., 2021), raising the possibility that interactions between RFX factors and Foxn3 or other forkhead factors could play important roles in CNS development.

Primary cilia in embryonic retinas from Foxn3-/- mice appear disorganized, with more structural variation than primary cilia in retinas from wild-type mice. Upregulated genes in the Foxn3-/- retinas include Ift88 and other cilia components that are involved in transport of components within cilia (Klena and Pigino, 2022), suggesting that disrupted or increased transport could contribute to the observed changes in cilia. Signaling pathways can be impacted by changes in transport within cilia (Christensen et al., 2017; Qin et al., 2011). Ciliopathies with altered ciliary transport or other defects in cilia can impact the retina, often affecting the modified cilium of photoreceptors. Since loss of Foxn3 is lethal near birth, it was not possible to evaluate possible requirements for Foxn3 in the mature retina. However, the disrupted transcriptional regulation of cilia genes in the Foxn3-/- retinas suggests that mutations in Foxn3 could be associated with cilopathies.

Foxn3 function has been implicated in the repression of cell growth, acting as a tumor suppressor, linked to the regulation of glucose metabolism in the liver, and can modulate inflammation in the lungs (Huot et al., 2014; Karanth et al., 2016; Li et al., 2017; Xue et al., 2019; Zhang et al., 2021; Zhu et al., 2023). Craniofacial defects have been reported in mice with a hypomorphic Foxn3 allele or after morpholino inhibition of Foxn3 in frogs (Samaan et al., 2010; Schmidt et al., 2011; Schuff et al., 2007), although the Foxn3-/- mice analyzed here do not have apparent craniofacial defects. The regulation of many genes involved in cilia by Foxn3 suggests that regulation of cilia could be important for some of these functions of Foxn3.

We previously found that Foxn3 and Foxn4 mRNAs are both expressed in retinal progenitor cells (Zhang et al., 2022). Since Foxn4 can bind to two intronic enhancers in the Foxn3 gene, and activate reporters based on those enhancers, it is possible that Foxn4, in cooperation with Ascl1 and other factors, helps to upregulate Foxn3 in retinal cells to prevent activation of the Foxj1 gene and its downstream targets in the motile cilia pathway. However, the Foxn3 mRNA was increased about two-fold in Foxn4-/- retinas (see Supplemental Table 2 in Liu et al., 2020), suggesting that other factors also influence Foxn3 expression. Foxn3 appears likely to repress its own expression, based on its ability to repress the two Foxn3 intronic enhancer reporters, potentially creating a negative feedback loop to limit Foxn3 expression levels.

We previously identified the Foxn3 mRNA as a target of miR-216b (Zhang et al., 2022). Overexpression of miR-216b or inhibition of Foxn3 expression in neonatal retinas, using in vivo electroporation, led to the formation of additional amacrine interneurons and loss of bipolar interneurons. We proposed a model in which inhibition of Foxn3 expression by miR-216b allowed increased Foxn4 activity to promote amacrine cell formation. Since Foxn3-/- die at birth, we could not perform similar postnatal analyses on the Foxn3 null retinas. However, the disruption of the Foxn3 gene did not lead to obvious changes in amacrine cells or other cell types present in the embryonic retinas at E19. Since Foxn3 is disrupted throughout development in Foxn3-/- mice, it is possible that compensation occurs in the Foxn3-/- retina, but similar compensation does not occur or is not rapid enough in the postnatal electroporation experiments. While mRNA for the related Foxn2 protein is expressed at a low level in retinas, there was no significant change in Foxn2

mRNA in Foxn3-/- retinas (Supplemental Table 1). Another possibility is that the mosaic nature of in vivo electroporation experiments could contribute to the observed phenotype. Electroporation delivers DNA into a subset of retinal precursor cells, and only those cells are later scored for cell fate. Reduced Foxn3 expression in the electroporated cells with normal Foxn3 still present in non-electroporated retinal cells may lead to cell fate changes that do not occur if Foxn3 is disrupted in all cells, perhaps via asymmetric cell-cell signaling (e.g., through the Notch pathway, see Del Barrio et al., 2007). Finally, we cannot rule out that the Foxn3 gene without exon 3 in Foxn3-/- mice retains partial function by producing a truncated Foxn3 protein. However, the lack of effect of the truncated Foxn3 protein in reporter assays suggests that these mice lack Foxn3 function.

It is not clear if the retinal phenotypes observed after postnatal electroporation of miR-216b could arise from changes to primary cilia. However, our PAR-CLIP experiments identified a miR-216b site in the 3' UTR of the Rfx3 mRNA in the P0 retina (see Supplemental Table 3 in Zhang et al. 2022), suggesting that miR-216b targets multiple regulators of cilia gene expression. Signaling by Shh and TGFβ, two pathways with receptors in primary cilia, have been reported to alter amacrine cell formation. Loss of the Shh inhibitor Suppressor of Fused during early retina development in the mouse leads most retinal precursor cells to differentiate as amacrine cells (Cwinn et al., 2011), while TGFβ signaling acts as feedback inhibitor for amacrine cell formation at later ages (Ma et al., 2007). One or both pathways could potentially be affected by miR-216b. However, not all genes with Foxn3 bound nearby are related to cilia formation or function, so it remains

possible that miR-216b acts through modulation of Foxn3 expression but independent from the role of Foxn3 in repressing genes associated with cilia.

Methods

Mice and processing of retinas

All mouse (*Mus musculus*) experiments were approved by the Institutional Animal Care & Use Committee at the University of Michigan. Wild-type retinas were isolated from embryonic day 16 (E16) embryos of CD-1 mice (Charles River). The C57BL/6NJ-*Foxn3*$^{em1(IMPC)Bay}$/Mmnc mouse strain (RRID:MMRRC_071094-UNC), was obtained from the Mutant Mouse Resource and Research Center (MMRRC) at University of North Carolina at Chapel Hill, an NIH-funded strain repository, and was donated to the MMRRC by Jason Heaney, Ph.D., Baylor College of Medicine (Birling et al., 2021). C57BL/6NJ-*Foxn3*$^{em1(IMPC)Bay}$/Mmnc mice were bred with wild-type C57/BL6J mice. The offspring, consisting of heterozygous males and females, were interbred. Retinas from homozygous and wild-type embryos were harvested at E19 and used for further experiments. The genotype of animals and embryos was determined by PCR using the primers:

Foxn3_WF, CGTTTCCATTTTTGTAAGATCG;

Foxn3_WR, ATGCACCACAATGACCCTTT;

Foxn3_MF, CATGAACGTCAGCCAAGACG;

Foxn3_MR, CCATCACTCAGGAGCCTGTC.

For tissue analysis, eyes were fixed with 2% paraformaldehyde (ThermoFisher) in phosphate-buffered saline (PBS, Sigma) for 30 min at room temperature and retinas were

dissected from the eyes. For sections, retinas were cryoprotected in PBS containing 30% sucrose (Sigma) for 2h at 4°C, and embedded in OCT (Sakura), prior to preparation of cryosections (16 μm) using a cryostat. All the retinas were processed similarly to obtain tissue for antibody staining.

Plasmids

Plasmids were constructed using standard techniques, with oligonucleotides for plasmid construction detailed in Supplemental Table 6. The plasmids pUS2, pUS2-Foxn3, and pUS2-Foxn4 have been previously described (Chung et al., 2006; Zhang et al., 2022). DNA oligonucleotides encoding a 2XHA tag were inserted into pUS2, pUS2-Foxn3, or pUS2-Foxn4 between the BamHI and EcoRI sites, resulting in pUS2-HA, pUS2-HA-Foxn3, and pUS2-HA-Foxn4. The coding regions for mouse Foxj1, Rfx3, and Foxn3 without exon 3 (from C57BL/6NJ-*Foxn3*$^{em1(IMPC)Bay}$/Mmnc mice) were isolated by RT-PCR, using RNA extracted from embryonic mouse retinas, and inserted into pUS2-HA and pUS2. The 7A mutants, with a seven-amino-acid Ala substitution of the LXXLXWL motif (LXXLXWL to AAAAAAA), were generated using PCR site-directed mutagenesis.

The enhancer or promoter regions of Foxn3, Tek1, Ccdc39, Cfap206, Notch1, Meis1, Foxj1, and Ptprf were amplified from mouse genomic DNA via PCR and cloned into pGL4.29 (Promega) using the NEBuilder HiFi DNA Assembly Cloning Kit (New England Biolabs). The Foxn3_Enh2_FBM construct, which contains mutations in two forkhead binding sites, and the Foxn3_Enh2_EBM construct, with mutations in two E-boxes, were created by inserting synthesized oligonucleotides into pGL4.29. Additionally, the Foxn3_Enh2_Rfx3M construct,

featuring mutations in the Rfx3 binding site, was generated using PCR site-directed mutagenesis.

RNAseq

Retinas from individual E19 embryos (Foxn3 knockout or wild type) were isolated, and total RNA from each retina was purified using TRIzol. A total of 500 ng of RNA was used to prepare the RNAseq library using the NEBNext Ultra™ II Directional RNA Library Prep Kit for Illumina and NEB Unique Dual Index UMI Adaptors (New England Biolabs), following the manufacturer's instructions. The RNAseq libraries were sequenced on an Illumina NextSeq at the University of Michigan Advanced Genomics Core.

CUT&RUN

E16 retinas from CD-1 mice were isolated, pooled, and dissociated into single cells using Accutase (Gibco). Approximately 3×10^5 cells were used for each CUT&RUN assay, which was performed using the CUT&RUN Assay Kit (Cell Signaling Technologies) following the manufacturer's instructions for live cell preparation. The genomic DNA recovered from the CUT&RUN assay was used to prepare a DNA library using the NEBNext Ultra II DNA Library Prep Kit for Illumina, adhering to the manufacturer's protocol with the following modification: after the addition of End Prep Buffer and Enzyme Mix, samples were incubated at 20°C for 30 minutes and subsequently at 50°C for 30 minutes.

For ligation, 2.5 µl of 1:50 diluted NEB Unique Dual Index UMI Adaptors were added. Adaptor-ligated DNA was purified using 1.1X volume of NEBNext Sample Purification

Beads. Following PCR enrichment, the adaptor-ligated DNA was again purified using 1.1X volume of beads. The PCR product was separated on a 6% TBE gel (Life Technologies), and a gel slice corresponding to 200–500 bp (determined using size markers in an adjacent lane) was excised. The DNA from the gel slice was eluted, precipitated using 2-propanol, resuspended in Tris-HCl buffer, and sequenced using an Illumina NextSeq at the University of Michigan Advanced Genomics Core.

Bioinformatic analysis

Paired-end RNAseq reads (50ntX2) were mapped to mm39 using star (Dobin et al., 2013). Differential expression of genes in RNAseq data was determined with DEseq2 (Love et al., 2014). For CUT&RUN analysis, 50ntX2 paired-end Illumina sequences had adaptors removed using Cutadapt (Martin, 2011) and were then mapped to mm10 mouse genome and to the Saccharomyces_cerevisiae genome (for yeast spike-in DNA) with bowtie2 (Langmead and Salzberg, 2012). Mapped reads were deduplicated based on UMIs using UMI-Tools (Smith et al., 2017). Paired-end reads were filtered for insert sizes of 120nt or less as recommended for transcription factor peak finding with CUT&RUN (Meers et al., 2019b; Meers et al., 2019c). Bedgraph files of read coverage for the mouse genome were generated using bedtools genomecov (Quinlan, 2014; Quinlan and Hall, 2010) and normalized based on total yeast spike in read counts for each library. Significant ($q<0.0001$) peaks of read accumulation were identified using SEACR with relaxed peak finding (Meers et al., 2019a). Peaks were identified from two independent CUT&RUN libraries for each transcription factor, relative to two matched IgG control libraries. For Foxn3, peaks

identified in two separate CUT&RUN experiments (each with two independent samples and two control samples) were intersected to generate a high confidence set of Foxn3 peaks that was used for subsequent Foxn3 binding region analysis.

The summit of each SEACR peak was defined as the center base in the region with the maximum read count. Peaks were filtered using exclude lists for CUT&RUN (Nordin et al., 2023) and ENCODE Chip-seq (Amemiya et al., 2019); non-chromosomal and chrM mappings also were discarded. Homer 5.1 (Heinz et al., 2010) was used to map DNA binding motifs in each peak. Peaks were linked to a gene annotation based on the nearest TSS from epdNewPromoter_v6.TSS (Dreos et al., 2012) for each peak summit, determined with bedtools closest. ENCODE cCREs (Abascal et al., 2020) that overlapped at least 10% of a SEACR peak were identified using bedtools intersect. Gene symbols for annotated CUT&RUN peaks were updated to current MGI symbols (https://www.informatics.jax.org/batch) and matched to the genes in the RNAseq data. Overlaps between peaks for different factors were determined using bedtools intersect with at least 10% overlap.

Heat maps for pooled or individual samples, centered on peak summits, were generated using Deep Tools (Ramirez et al., 2016). Graphic displays of read mapping were generated with IGV (Thorvaldsdottir et al., 2013). Volcano plots were generated with VolcaNoseR (Goedhart and Luijsterburg, 2020). Venn diagrams were generated via the Broad Institute Venn diagram generator (http://barc.wi.mit.edu/tools/). GO analysis was performed using the NIH DAVID web site (https://david.ncifcrf.gov/tools.jsp). Figures were labeled with Adobe Illustrator.

Reporter Assays

HEK293 cells were cultured in 96-well plates in DMEM supplemented with 10% fetal bovine serum (FBS), 100 units/ml penicillin, and 100 µg/ml streptomycin (all from ThermoFisher). For each well, 20 ng of reporter DNA (Foxn3Enh2_WT, Foxn3Enh2_RfxM, Foxn3Enh2_FBM, Foxn3Enh2_EBM, Foxn3Enh1, Tek1, Ccdc39, Cfap206, Foxj1, Meis1, Notch1 or Ptprf) was co-transfected with 20 ng of either individual or combinations of the following DNA constructs: pUS2, pUS2-Foxn3, pUS2-Foxn3_7A, pUS2-Foxn4, pUS2-Foxn4_7A, pUS2-Foxj, pUS2-Ascl1, or pUS2-Rfx3. An additional 20 ng of pRL-SV40 was included as an internal control for transfection efficiency. Transfections were carried out using Lipofectamine 2000 (ThermoFisher) following the manufacturer's protocol.

Reporter activity was measured 24 hours post-transfection using the Dual-Glo® Luciferase Assay System (Promega). Firefly luciferase activity was normalized to Renilla luciferase activity to account for transfection efficiency. Luminescence intensity was measured with a FLUOstar OPTIMA plate reader. The relative expression data shown in the figures represent the mean from 3-6 independent transfections (biological replicates). Individual data points for each independent transfection show the mean of technical assay replicates. Statistical analysis was performed using 2-way ANOVA with GraphPad Prism 10.

Co-immunoprecipitation and Western Blot Analyses

In 10-cm dishes, 2 µg of pUS2-Rfx3 plasmid was co-transfected into HEK293 cells along with 2 µg of either pUS2-HA-Foxn3, pUS2-HA-Foxn3-7A, pUS2-HA-Foxn4, pUS2-HA-Foxn4-

7A, pUS2-HA-FoxJ1, or pUS2-HA-FoxJ1-7A. Transfections were performed using Lipofectamine 2000 following the manufacturer's protocol. Protein extracts were prepared 24 hours post-transfection in NETN buffer (20 mM Tris-HCl, pH 8.0 (Invitrogen), 100 mM NaCl (Lonza), 0.5% NP-40 (Sigma), 0.5 mM EDTA(Invitrogen)) supplemented with a protease and phosphatase inhibitor cocktail (Sigma). The lysates were centrifuged at 13,000 rpm for 5 minutes at 4°C.

For immunoprecipitation, 20 µL of Pierce™ Anti-HA Magnetic Beads were incubated with the cell lysates for 2 hours at 4°C with constant rotation. After incubation, the beads were washed three times with NETN buffer. The precipitated proteins were then eluted by resuspending the beads in 1x NuPAGE LDS loading buffer and boiling for 10 minutes. The immunoprecipitated proteins or cell lysates were separated using 10% NuPAGE gels and transferred to nitrocellulose membranes (All Invitrogen). For Western blot analysis, rabbit anti-HA (1:2000, Cell Signaling Technology) and rabbit anti-Rfx3 (1:1000, Sigma) were used as primary antibodies. The secondary antibody, IRDye800CW goat anti-rabbit (1:8000), was obtained from Li-COR. Western blots were visualized using the Bio-Rad ChemiDoc MP Imaging System.

Immunofluorescence Analysis

Retina sections were treated with a blocking solution (1% unlabeled affinity-purified Fab fragment donkey anti-mouse IgG (H+L) and 5% donkey serum (Jackson Immunoresearch) in PBS containing 0.1% Triton X-100 (ThermoFisher)) at room temperature for 1 hour. The sections were then incubated overnight at 4°C with mouse anti-AP2α. Following this,

sections were incubated for 1 hour at room temperature with Alexa Fluor 647-conjugated anti-mouse secondary antibody (1:1000, Jackson Immunoresearch). After antibody staining, Hoechst 33342 (Roche) was used to counterstain the nuclei. Immunofluorescence was imaged on an Olympus FV3000 confocal microscope, and images were analyzed with FV10-ASW 3.1 Viewer, where colors were assigned. For whole-mount preparations, fixed retinas were processed with blocking solution at room temperature for 2 hours, followed by primary antibody incubation overnight at 4°C with mouse anti-Arl13b and rabbit anti-IFT88. Secondary antibody incubation (Alexa Fluor 647-conjugated anti-mouse and Alexa Fluor 568-conjugated anti-rabbit (1:1000, Jackson Immunoresearch)) was performed for 2 hours at room temperature. Hoechst 33342 (Roche) was used to counterstain the nuclei. Retinas were flat-mounted in PBS, and immunofluorescence was imaged on an Oxford Andor BC43 microscope. Images were analyzed, and colors were assigned using Imaris Viewer 10.2.0 or FIJI.

For both sections and whole-mount preparations, representative images were cropped, assembled, and labeled using Adobe Photoshop and/or Adobe Illustrator.

Acknowledgements

We thank Andrew Tidball and Jack Parent for assistance with microscopy. We thank Jillian Pearring for helpful discussions, antibodies, and assistance with microscopy. We thank Anne Vojtek for helpful discussions and comments on the manuscript; we thank Mike Uhler for helpful discussions.

Funding

Supported by R01 EY02499 from the National Institutes of Health/National Eye Institute, and grants from the University of Michigan Biomedical Research Council and the University of Michigan Office of Research (D.L.T.). This work utilized the Vision Research Core at the University of Michigan Kellogg Eye Center, which is supported by National Institutes of Health/National Eye Institute P30 EY007003.

References

Abascal, F., Acosta, R., Addleman, N. J., Adrian, J., Afzal, V., Ai, R., Aken, B., Akiyama, J. A., Jammal, O. A., Amrhein, H., et al. (2020). Expanded encyclopaedias of DNA elements in the human and mouse genomes. *Nature* **583**, 699-710.

Amemiya, H. M., Kundaje, A. and Boyle, A. P. (2019). The ENCODE Blacklist: Identification of Problematic Regions of the Genome. *Scientific Reports* **9**, 9354.

Beckers, A., Adis, C., Schuster-Gossler, K., Tveriakhina, L., Ott, T., Fuhl, F., Hegermann, J., Boldt, K., Serth, K., Rachev, E., et al. (2020). The FOXJ1 target Cfap206 is required for sperm motility, mucociliary clearance of the airways and brain development. *Development* **147**.

Berkes, C. A., Bergstrom, D. A., Penn, B. H., Seaver, K. J., Knoepfler, P. S. and Tapscott, S. J. (2004). Pbx Marks Genes for Activation by MyoD Indicating a Role for a Homeodomain Protein in Establishing Myogenic Potential. *Molecular Cell* **14**, 465-477.

Birling, M.-C., Yoshiki, A., Adams, D. J., Ayabe, S., Beaudet, A. L., Bottomley, J., Bradley, A., Brown, S. D. M., Bürger, A., Bushell, W., et al. (2021). A resource of targeted mutant mouse lines for 5,061 genes. *Nature Genetics* **53**, 416-419.

Boehm, T., Bleul, C. C. and Schorpp, M. (2003). Genetic dissection of thymus development in mouse and zebrafish. *Immunol. Rev.* **195**, 15-27.

Boudreau-Pinsonneault, C., David, L. A., Lourenco Fernandes, J. A., Javed, A., Fries, M., Mattar, P. and Cayouette, M. (2023). Direct neuronal reprogramming by temporal identity factors. *Proc Natl Acad Sci U S A* **120**, e2122168120.

Brocal-Ruiz, R., Esteve-Serrano, A., Mora-Martínez, C., Franco-Rivadeneira, M. L., Swoboda, P., Tena, J. J., Vilar, M. and Flames, N. (2023). Forkhead transcription factor FKH-8 cooperates with RFX in the direct regulation of sensory cilia in Caenorhabditis elegans. *eLife* **12**, e89702.

Burnett, J. B., Lupu, F. I. and Eggenschwiler, J. T. (2017). Proper ciliary assembly is critical for restricting Hedgehog signaling during early eye development in mice. *Dev Biol* **430**, 32-40.

Campbell, E. P., Quigley, I. K. and Kintner, C. (2016). Foxn4 promotes gene expression required for the formation of multiple motile cilia. *Development (Cambridge, England)* **143**, 4654-4664.

Chen, H. Y., Kelley, R. A., Li, T. and Swaroop, A. (2021). Primary cilia biogenesis and associated retinal ciliopathies. *Semin. Cell Dev. Biol.* **110**, 70-88.

Chi, N. C., Shaw, R. M., De Val, S., Kang, G., Jan, L. Y., Black, B. L. and Stainier, D. Y. (2008). Foxn4 directly regulates tbx2b expression and atrioventricular canal formation. *Genes Dev* **22**, 734-739.

Choksi, S. P., Lauter, G., Swoboda, P. and Roy, S. (2014). Switching on cilia: transcriptional networks regulating ciliogenesis. *Development* **141**, 1427-1441.

Christensen, S. T., Morthorst, S. K., Mogensen, J. B. and Pedersen, L. B. (2017). Primary Cilia and Coordination of Receptor Tyrosine Kinase (RTK) and Transforming Growth Factor β (TGF-β) Signaling. *Cold Spring Harb. Perspect. Biol.* **9**, a028167.

Chung, K.-H., Hart, C. C., Al-Bassam, S., Avery, A., Taylor, J., Patel, P. D., Vojtek, A. B. and Turner, D. L. (2006). Polycistronic RNA polymerase II expression vectors for RNA interference based on BIC/miR-155. *Nucleic acids research* **34**, e53 - e53.

Cwinn, M. A., Mazerolle, C., McNeill, B., Ringuette, R., Thurig, S., Hui, C. c. and Wallace, V. A. (2011). Suppressor of Fused Is Required to Maintain the Multipotency of Neural Progenitor Cells in the Retina. *Journal of Neuroscience* **31**, 5169-5180.

Del Barrio, M. G., Taveira-Marques, R., Muroyama, Y., Yuk, D.-I., Li, S., Wines-Samuelson, M., Shen, J., Smith, H. K., Xiang, M., Rowitch, D., et al. (2007). A regulatory network involving Foxn4, Mash1 and delta-like 4/Notch1 generates V2a and V2b spinal interneurons from a common progenitor pool. *Development (Cambridge, England)* **134**, 3427-3436.

Derderian, C., Canales, G. I. and Reiter, J. F. (2023). Seriously cilia: A tiny organelle illuminates evolution, disease, and intercellular communication. *Developmental Cell* **58**, 1333-1349.

Didon, L., Zwick, R. K., Chao, I. W., Walters, M. S., Wang, R., Hackett, N. R. and Crystal, R. G. (2013). RFX3 Modulation of FOXJ1 regulation of cilia genes in the human airway epithelium. *Respir. Res.* **14**, 70.

Dilan, T. L., Moye, A. R., Salido, E. M., Saravanan, T., Kolandaivelu, S., Goldberg, A. F. X. and Ramamurthy, V. (2019). ARL13B, a Joubert Syndrome-Associated Protein, Is Critical for Retinogenesis and Elaboration of Mouse Photoreceptor Outer Segments. *J. Neurosci.* **39**, 1347-1364.

Dobin, A., Davis, C. A., Schlesinger, F., Drenkow, J., Zaleski, C., Jha, S., Batut, P., Chaisson, M. and Gingeras, T. R. (2013). STAR: ultrafast universal RNA-seq aligner. *Bioinformatics* **29**, 15-21.

Dreos, R., Ambrosini, G., Périer, R. C. and Bucher, P. (2012). EPD and EPDnew, high-quality promoter resources in the next-generation sequencing era. *Nucleic Acids Research* **41**, D157-D164.

Dubaic, M., Peskova, L., Hampl, M., Weissova, K., Celiker, C., Shylo, N. A., Hruba, E., Kavkova, M., Zikmund, T., Weatherbee, S. D., et al. (2023). Role of ciliopathy protein TMEM107 in eye development: insights from a mouse model and retinal organoid. *Life Science Alliance* **6**, e202302073.

Fiore, L., Takata, N., Acosta, S., Ma, W., Pandit, T., Oxendine, M. and Oliver, G. (2020). Optic vesicle morphogenesis requires primary cilia. *Developmental Biology* **462**, 119-128.

Goedhart, J. and Luijsterburg, M. S. (2020). VolcaNoseR is a web app for creating, exploring, labeling and sharing volcano plots. *Sci Rep* **10**, 20560.

Harris, H. K., Nakayama, T., Lai, J., Zhao, B., Argyrou, N., Gubbels, C. S., Soucy, A., Genetti, C. A., Suslovitch, V., Rodan, L. H., et al. (2021). Disruption of RFX family transcription factors causes autism, attention-deficit/hyperactivity disorder, intellectual disability, and dysregulated behavior. *Genet. Med.* **23**, 1028-1040.

Heinz, S., Benner, C., Spann, N., Bertolino, E., Lin, Y. C., Laslo, P., Cheng, J. X., Murre, C., Singh, H. and Glass, C. K. (2010). Simple combinations of lineage-determining transcription factors prime cis-regulatory elements required for macrophage and B cell identities. *Mol Cell* **38**, 576-589.

Herman, L., Todeschini, A.-L. and Veitia, R. A. (2021). Forkhead Transcription Factors in Health and Disease. *Trends in Genetics* **37**, 460-475.

Huot, G., Vernier, M., Bourdeau, V., Doucet, L., Saint-Germain, E., Gaumont-Leclerc, M.-F., Moro, A. and Ferbeyre, G. (2014). CHES1/FOXN3 regulates cell proliferation by repressing PIM2 and protein biosynthesis. *Molecular biology of the cell* **25**, 554-565.

Huttlin, E. L., Bruckner, R. J., Navarrete-Perea, J., Cannon, J. R., Baltier, K., Gebreab, F., Gygi, M. P., Thornock, A., Zarraga, G., Tam, S., et al. (2021). Dual proteome-scale networks reveal cell-specific remodeling of the human interactome. *Cell* **184**, 3022-3040 e3028.

Huttlin, E. L., Bruckner, R. J., Paulo, J. A., Cannon, J. R., Ting, L., Baltier, K., Colby, G., Gebreab, F., Gygi, M. P., Parzen, H., et al. (2017). Architecture of the human interactome defines protein communities and disease networks. *Nature* **545**, 505-509.

Islam, M. M., Li, Y., Luo, H., Xiang, M. and Cai, L. (2013). Meis1 regulates Foxn4 expression during retinal progenitor cell differentiation. *Biology open* **2**, 1125-1136.

Iwama, A., Pan, J., Zhang, P., Reith, W., Mach, B., Tenen, D. G. and Sun, Z. (1999). Dimeric RFX Proteins Contribute to the Activity and Lineage Specificity of the Interleukin-5 Receptor α Promoter through Activation and Repression Domains. *Molecular and Cellular Biology* **19**, 3940-3950.

Karanth, S., Chaurasia, B., Bowman, F. M., Tippetts, T. S., Holland, W. L., Summers, S. A. and Schlegel, A. (2019). FOXN3 controls liver glucose metabolism by regulating gluconeogenic substrate selection. *Physiol. Rep.* **7**, e14238.

Karanth, S., Zinkhan, E. K., Hill, J. T., Yost, H. J. and Schlegel, A. (2016). FOXN3 Regulates Hepatic Glucose Utilization. *Cell Rep* **15**, 2745-2755.

Klena, N. and Pigino, G. (2022). Structural Biology of Cilia and Intraflagellar Transport. *Annual Review of Cell and Developmental Biology* **38**, 103-123.

Kowal, T. J., Dhande, O. S., Wang, B., Wang, Q., Ning, K., Liu, W., Berbari, N. F., Hu, Y. and Sun, Y. (2022). Distribution of prototypical primary cilia markers in subtypes of retinal ganglion cells. *J. Comp. Neurol.* **530**, 2176-2187.

Langmead, B. and Salzberg, S. L. (2012). Fast gapped-read alignment with Bowtie 2. *Nat Methods* **9**, 357-359.

Lemeille, S., Paschaki, M., Baas, D., Morle, L., Duteyrat, J. L., Ait-Lounis, A., Barras, E., Soulavie, F., Jerber, J., Thomas, J., et al. (2020). Interplay of RFX transcription factors 1, 2 and 3 in motile ciliogenesis. *Nucleic Acids Res* **48**, 9019-9036.

Li, S., Mo, Z., Yang, X., Price, S. M., Shen, M. M. and Xiang, M. (2004). Foxn4 controls the genesis of amacrine and horizontal cells by retinal progenitors. *Neuron* **43**, 795-807.

Li, W., Zhang, Z., Liu, X., Cheng, X., Zhang, Y., Han, X., Zhang, Y., Liu, S., Yang, J., Xu, B., et al. (2017). The FOXN3-NEAT1-SIN3A repressor complex promotes progression of hormonally responsive breast cancer. *Journal of Clinical Investigation* **127**, 3421-3440.

Li, X., Wang, W., Wang, J., Malovannaya, A., Xi, Y., Li, W., Guerra, R., Hawke, D. H., Qin, J. and Chen, J. (2015). Proteomic analyses reveal distinct chromatin-associated and soluble transcription factor complexes. *Molecular Systems Biology* **11**, 775.

Liu, S., Liu, X., Li, S., Huang, X., Qian, H., Jin, K. and Xiang, M. (2020). Foxn4 is a temporal identity factor conferring mid/late-early retinal competence and involved in retinal synaptogenesis. *Proceedings of the National Academy of Sciences* **85**, 201918628.

Love, M. I., Huber, W. and Anders, S. (2014). Moderated estimation of fold change and dispersion for RNA-seq data with DESeq2. *Genome biology* **15**, 550.

Luo, H., Jin, K., Xie, Z., Qiu, F., Li, S., Zou, M., Cai, L., Hozumi, K., Shima, D. T. and Xiang, M. (2012). Forkhead box N4 (Foxn4) activates Dll4-Notch signaling to suppress photoreceptor cell fates of early retinal progenitors. *Proceedings of the National Academy of Sciences of the United States of America* **109**, E553-E562.

Lyu, P., Iribarne, M., Serjanov, D., Zhai, Y., Hoang, T., Campbell, L. J., Boyd, P., Palazzo, I., Nagashima, M., Silva, N. J., et al. (2023). Common and divergent gene regulatory networks control injury-induced and developmental neurogenesis in zebrafish retina. *Nat Commun* **14**, 8477.

Ma, L., Cantrup, R., Varrault, A., Colak, D., Klenin, N., Götz, M., McFarlane, S., Journot, L. and Schuurmans, C. (2007). Zac1 functions through TGFβII to negatively regulate cell number in the developing retina. *Neural Development* **2**, 11.

Martin, M. (2011). Cutadapt removes adapter sequences from high-throughput sequencing reads. *EMBnet.journal* **17**, pp. 10-12.

Meers, M. P., Bryson, T. and Henikoff, S. (2019a). A streamlined protocol and analysis pipeline for CUT&RUN chromatin profiling. *bioRxiv* **362**, 569129.

Meers, M. P., Bryson, T. D., Henikoff, J. G. and Henikoff, S. (2019b). Improved CUT&RUN chromatin profiling tools. *eLife* **8**, e46314.

Meers, M. P., Tenenbaum, D. and Henikoff, S. (2019c). Peak calling by Sparse Enrichment Analysis for CUT&RUN chromatin profiling. *Epigenetics Chromatin* **12**, 42.

Misra, K., Luo, H., Li, S., Matise, M. and Xiang, M. (2014). Asymmetric activation of Dll4-Notch signaling by Foxn4 and proneural factors activates BMP/TGFβ signaling to specify V2b interneurons in the spinal cord. *Development (Cambridge, England)* **141**, 187-198.

Nakagawa, S., Gisselbrecht, S. S., Rogers, J. M., Hartl, D. L. and Bulyk, M. L. (2013). DNA-binding specificity changes in the evolution of forkhead transcription factors. *Proc Natl Acad Sci U S A* **110**, 12349-12354.

Nakayama, A., Murakami, H., Maeyama, N., Yamashiro, N., Sakakibara, A., Mori, N. and Takahashi, M. (2003). Role for RFX Transcription Factors in Non-neuronal Cell-specific Inactivation of the Microtubule-associated Protein MAP1A Promoter*. *Journal of Biological Chemistry* **278**, 233-240.

Ning, K., Sendayen, B. E., Kowal, T. J., Wang, B., Jones, B. W., Hu, Y. and Sun, Y. (2021). Primary Cilia in Amacrine Cells in Retinal Development. *Investigative Ophthalmology & Visual Science* **62**, 15.

Nordin, A., Zambanini, G., Pagella, P. and Cantù, C. (2023). The CUT&RUN suspect list of problematic regions of the genome. *Genome Biology* **24**, 185.

Pati, D., Keller, C., Groudine, M. and Plon, S. E. (1997). Reconstitution of a MEC1-independent checkpoint in yeast by expression of a novel human fork head cDNA. *Mol Cell Biol* **17**, 3037-3046.

Patir, A., Fraser, A. M., Barnett, M. W., McTeir, L., Rainger, J., Davey, M. G. and Freeman, T. C. (2020). The transcriptional signature associated with human motile cilia. *Scientific Reports* **10**, 10814.

Qin, J., Lin, Y., Norman, R. X., Ko, H. W. and Eggenschwiler, J. T. (2011). Intraflagellar transport protein 122 antagonizes Sonic Hedgehog signaling and controls ciliary localization of pathway components. *Proc Natl Acad Sci U S A* **108**, 1456-1461.

Quigley, I. K. and Kintner, C. (2017). Rfx2 Stabilizes Foxj1 Binding at Chromatin Loops to Enable Multiciliated Cell Gene Expression. *PLoS Genetics* **13**, e1006538.

Quinlan, A. R. (2014). BEDTools: The Swiss-Army Tool for Genome Feature Analysis. *Current protocols in bioinformatics / editoral board, Andreas D. Baxevanis ... [et al.]* **47**, 11 12 11-34.

Quinlan, A. R. and Hall, I. M. (2010). BEDTools: a flexible suite of utilities for comparing genomic features. *Bioinformatics* **26**, 841-842.

Ramirez, F., Ryan, D. P., Gruning, B., Bhardwaj, V., Kilpert, F., Richter, A. S., Heyne, S., Dundar, F. and Manke, T. (2016). deepTools2: a next generation web server for deep-sequencing data analysis. *Nucleic Acids Res* **44**, W160-165.

Rogers, J. M., Waters, C. T., Seegar, T. C. M., Jarrett, S. M., Hallworth, A. N., Blacklow, S. C. and Bulyk, M. L. (2019). Bispecific Forkhead Transcription Factor FoxN3 Recognizes Two Distinct Motifs with Different DNA Shapes. *Molecular cell*.

Samaan, G., Yugo, D., Rajagopalan, S., Wall, J., Donnell, R., Goldowitz, D., Gopalakrishnan, R. and Venkatachalam, S. (2010). Foxn3 is essential for craniofacial development in mice and a putative candidate involved in human congenital craniofacial defects. *Biochem Biophys Res Commun* **400**, 60-65.

Schmidt, J., Schuff, M. and Olsson, L. (2011). A role for FoxN3 in the development of cranial cartilages and muscles in Xenopus laevis (Amphibia: Anura: Pipidae) with special emphasis on the novel rostral cartilages. *J Anat* **218**, 226-242.

Schuff, M., Rössner, A., Wacker, S. A., Donow, C., Gessert, S. and Knöchel, W. (2007). FoxN3 is required for craniofacial and eye development of Xenopus laevis. *Developmental dynamics : an official publication of the American Association of Anatomists* **236**, 226-239.

Scott, K. L. and Plon, S. E. (2005). CHES1/FOXN3 interacts with Ski-interacting protein and acts as a transcriptional repressor. *Gene* **359**, 119-126.

Skene, P. J. and Henikoff, S. (2017). An efficient targeted nuclease strategy for high-resolution mapping of DNA binding sites. *Elife* **6**.

Smith, T., Heger, A. and Sudbery, I. (2017). UMI-tools: modeling sequencing errors in Unique Molecular Identifiers to improve quantification accuracy. *Genome Res* **27**, 491-499.

Song, J., Li, L., Fang, Y., Lin, Y., Wu, L., Wan, W., Wei, G., Hua, F. and Ying, J. (2023). FOXN Transcription Factors: Regulation and Significant Role in Cancer. *Molecular Cancer Therapeutics*, OF1-OF12.

Stauber, M., Weidemann, M., Dittrich-Breiholz, O., Lobschat, K., Alten, L., Mai, M., Beckers, A., Kracht, M. and Gossler, A. (2017). Identification of FOXJ1 effectors during ciliogenesis in the foetal respiratory epithelium and embryonic left-right organiser of the mouse. *Developmental Biology* **423**, 170-188.

Sugiaman-Trapman, D., Vitezic, M., Jouhilahti, E.-M., Mathelier, A., Lauter, G., Misra, S., Daub, C. O., Kere, J. and Swoboda, P. (2018). Characterization of the human RFX transcription factor family by regulatory and target gene analysis. *BMC Genomics* **19**, 181.

Swann, J. B., Weyn, A., Nagakubo, D., Bleul, C. C., Toyoda, A., Happe, C., Netuschil, N., Hess, I., Haas-Assenbaum, A., Taniguchi, Y., et al. (2014). Conversion of the thymus into a bipotent lymphoid organ by replacement of FOXN1 with its paralog, FOXN4. *Cell Rep* **8**, 1184-1197.

Thorvaldsdottir, H., Robinson, J. T. and Mesirov, J. P. (2013). Integrative Genomics Viewer (IGV): high-performance genomics data visualization and exploration. *Brief Bioinform* **14**, 178-192.

Vij, S., Rink, J. C., Ho, H. K., Babu, D., Eitel, M., Narasimhan, V., Tiku, V., Westbrook, J., Schierwater, B. and Roy, S. (2012). Evolutionarily Ancient Association of the FoxJ1 Transcription Factor with the Motile Ciliogenic Program. *PLoS Genetics* **8**, e1003019.

Wang, Y., Dakubo, G. D., Thurig, S., Mazerolle, C. J. and Wallace, V. A. (2005). Retinal ganglion cell-derived sonic hedgehog locally controls proliferation and the timing of RGC development in the embryonic mouse retina. *Development* **132**, 5103-5113.

Xue, W., Ma, L., Wang, Z., Zhang, W. and Zhang, X. (2019). FOXN3 is downregulated in osteosarcoma and transcriptionally regulates SIRT6, and suppresses migration and invasion in osteosarcoma. *Oncology Reports* **41**, 1404-1414.

Yu, X., Ng, C. P., Habacher, H. and Roy, S. (2008). Foxj1 transcription factors are master regulators of the motile ciliogenic program. *Nature Genetics* **40**, 1445-1453.

Zhang, H., Zhuang, P., Welchko, R. M., Dai, M., Meng, F. and Turner, D. L. (2022). Regulation of retinal amacrine cell generation by miR-216b and Foxn3. *Development* **149**.

Zhang, J., Hu, Z., Wen, C., Liao, Q., He, B., Peng, J., Tang, X., Chen, Z. and Xie, Y. (2021). MicroRNA-182 promotes epithelial-mesenchymal transition by targeting FOXN3 in gallbladder cancer. *Oncol Lett* **21**, 200.

Zhang, X. M. and Yang, X. J. (2001). Regulation of retinal ganglion cell production by Sonic hedgehog. *Development* **128**, 943-957.

Zhu, X., Huang, B., Zhao, F., Lian, J., He, L., Zhang, Y., Ji, L., Zhang, J., Yan, X., Zeng, T., et al. (2023). p38-mediated FOXN3 phosphorylation modulates lung inflammation and injury through the NF-κB signaling pathway. *Nucleic Acids Research*.

Žuklys, S., Handel, A., Zhanybekova, S., Govani, F., Keller, M., Maio, S., Mayer, C. E., Teh, H. Y., Hafen, K., Gallone, G., et al. (2016). Foxn1 regulates key target genes essential for T cell development in postnatal thymic epithelial cells. *Nature Immunology* **17**, 1206-1215.

Figure legends

Figure 1. Analysis of Foxn3-/- retinas. E19 Retinas from wild-type (A, B) and Foxn3-/- (C, D) do not show obvious differences in overall structure or amacrine cells (identified by expression of the AP2α protein: cyan; DNA/nuclei: blue). Volcano plot (E) for RNAseq analysis of E19 Foxn3-/- retinas relative to wild-type retinas shows that most of 930 differentially expressed genes ($q<0.0001$) are upregulated in the Foxn3-/- retinas. mRNAs significantly upregulated at least two-fold are indicated in magenta, while at least two-fold significantly downregulated mRNAs are labeled in dark blue. For Tekt1 and Foxj1 q=0; $-\log_{10}$ q was set to 250 for these two genes. (D) GO analysis of differentially expressed genes reveals enrichment for multiple GO categories related to cilia. Labeled mRNAs in (E) have been linked to cilia, except for Gja8, Lrrc10b, and Slc15a2.

Figure 2. Altered primary cilia in the developing retina in the absence of Foxn3. (A-C) Immunofluorescence detection of Arl13b (green) and Ift88 (magenta) in primary cilia at the outer surface of a representative whole-mount E19 wild-type retina. Maximum intensity projection of top 6μm of the retina (Z axis). DNA/nuclei: blue. (A'-C') Maximum intensity projection for 3μm virtual transverse section (Y axis) through the retina cilia; the boundaries of the section are indicated by yellow lines in A-C. (D-F) Primary cilia at the outer surface of a representative whole-mount E19 Fox3-/- retina, with 3μm virtual transverse section (D'-F'), details as for A-C/A'-C'. Primary cilia are disorganized and have more variable expression of Ift88 in the Foxn3-/- retina when compared to the wild-type retina. Scale bars (3μm) in A' and D' apply to all panels.

Figure 3. Analysis of Foxn3 genomic binding in the developing retina. (A) Heat map of read coverage at consistent Foxn3 binding regions identified by CUT&RUN in E16 retinas. Two anti-Foxn3 samples and two IgG control samples are shown for each of two experiments. (B) Most Foxn3 binding regions overlap Encode cCREs annotated as promoters or enhancers. (C) Venn diagram of overlap between differentially expressed genes in Foxn3-/- retinas and genes with Foxn3 binding sites identified by CUT&RUN. (D) CUT&RUN read peaks at the Foxj1 promoter. The range of read counts is indicated. (E) FHL and FKH forkhead binding motifs are enriched in the Foxn3 binding regions. In addition, motifs for RFX transcription factors are enriched in the Foxn3 binding regions.

Figure 4. Foxn3 represses reporters for cilia genes. (A) CUT&RUN read coverage for three genes encoding proteins that function in primary cilia. Foxn3 binding regions are present at the promoters in E16 retinas. The range for read coverage for each sample is indicated. Graphs showing activation of transfected Luciferase reporters, based on the promoter regions from Ccdc39 (B), Tekt1 (C), or Cfap206 (D), by cotransfection of Foxj1 in HEK293 cells, relative to the US2 control vector, with or without cotransfection of either an Rfx3 expression vector or the US2 control vector. Reporter activation was blocked by co-expression of Foxn3. N=3-6 for each sample, with standard deviations indicated. **** $q \leq 0.0001$, * $q \leq 0.05$.

Figure 5. Analysis of Rfx3 and Foxn4 genomic binding in the developing retina. (A) Heat map showing Rfx3 binding regions identified by CUT&RUN. Most Foxn3 binding regions overlap with Rfx3 binding regions. (B) Heat map showing Foxn4 binding regions identified by CUT&RUN. Many Foxn4 binding regions overlap with Foxn3 binding regions. (C) Venn diagram showing overlaps among Foxn3, Rfx3, and Foxn4 binding regions. (D) Rfx3 (dimeric) and Rfx7 (monomeric) binding motifs are enriched in the Rfx3 bound regions. FHL motifs are enriched in the Foxn4 bound regions. (E) In E16 retinas, the Foxj1 promoter region is bound by Foxn3 and by Rfx3, but not by Foxn4. Locations of Rfx3 or FHL/FKH motifs are indicated. (F) A Luciferase reporter based on the Foxj1 promoter is cooperatively activated by Foxn4 and Rfx3 in HEK293 cells, while co-expression of Foxn3 prevents activation of the reporter. Labels as in Fig. 4.

Figure 6. Regulation of reporters by Foxn4, Rfx3, and Foxn3. Luciferase reporters were constructed for various promoters or intronic enhancers bound by Foxn3 in the retina, and the reporters were assayed in HEK293 cells (see text). (A) The Ptprf enhancer is cooperatively activated by Foxn4 and Rfx3, while co-expressed Foxn3 inhibits activation. Enhancers from Meis1 (B) and Notch1 (C) are activated by Foxn4 but are not effectively repressed by Foxn3. Two intronic enhancers in the Foxn3 gene are bound by Foxn3, Rfx3, and Foxn4 in the retina (E). Reporters based on either enhancer are cooperatively activated by Foxn4 and Rfx3, and efficiently repressed by Foxn3 in transfection assays (D, F). Potential binding site motifs for Rfx3, Ascl1 (E-boxes), or Foxn3/Foxn4 are indicated (E). Reporters with mutations in the binding motifs were assayed. Disruption of the two E-boxes

(G) prevented Ascl1 cooperation with Foxn4, but did not alter the effects of Foxn4 or Foxn3. Mutation of the FKH and FHL-N sites (H) greatly reduced but did not abolish activation by Foxn4 and reduced inhibition by Foxn3, with or without Rfx3. Mutation of the Rfx3 site (I) reduced reporter activation, although Foxn4 + Ascl1 +/- Rfx3 still activated weakly. Foxn3 repression was abolished by mutation of the Rfx3 site. *** q≤0.001; Other labels as in Fig. 4.

Figure 7. A protein motif required for complex formation between Rfx3 and Foxn3, Foxn4, or Foxj1. (A) Schematic showing the location of a novel LXXLXWL motif present in the C. elegans FKH-8 protein and several mouse forkhead transcription factors, including Foxn3, Foxn4, and Foxj1 (see text). (B) Western blot (WB) showing epitope tagged HA-Foxn4, HA-Foxj1, or HA-Foxn3 co-immunoprecipitate (IP) with Rfx3 when expressed in HEK293 cells. Substitution of the LXXLXWL motif with 7 alanines in Foxn3-7A, Foxn4-7A, or Foxj1-7A (A) prevents co-immunoprecipitation with Rfx3. (C) Foxn4-7A has reduced reporter activation compared to Foxn4. In contrast to Foxn3, Foxn3-7A fails to inhibit activation of the reporter.

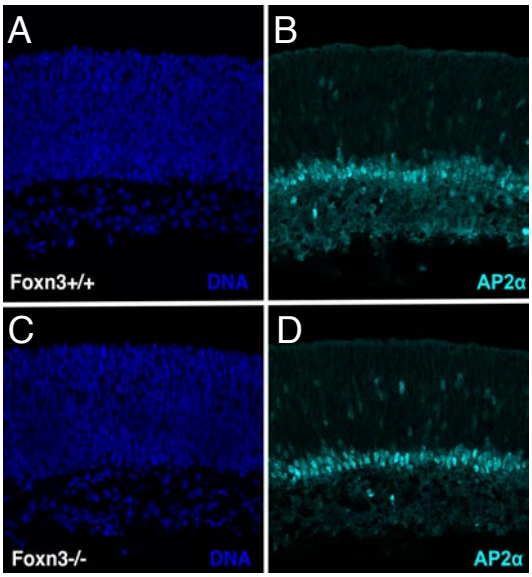
A
B
C
D
Foxn3+/+
DNA
AP2α
Foxn3-/-
DNA
AP2α

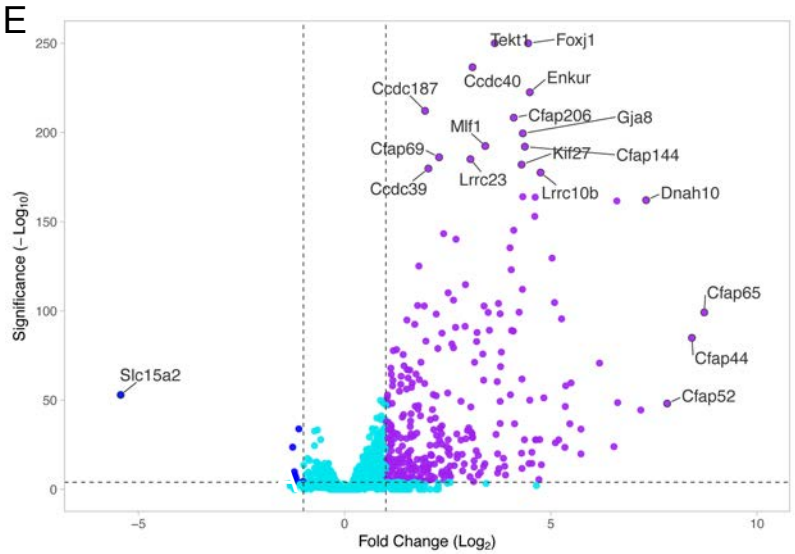
E
Tekt1
Foxj1
Ccdc40
Enkur
Ccdc187
Cfap206
Gja8
Mlf1
Cfap69
Kif27
Cfap144
Lrrc23
Ccdc39
Lrrc10b
Dnah10
Cfap65
Cfap44
Slc15a2
Cfap52
Significance (−Log10)
Fold Change (Log2)
250
200
150
100
50
0
−5
0
5
10

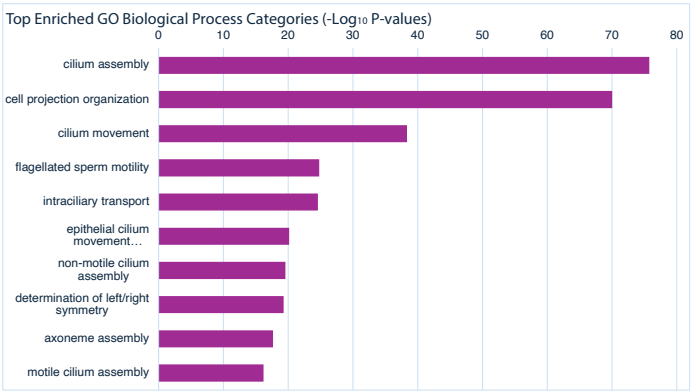
F
Top Enriched GO Biological Process Categories (-Log10 P-values)
0
10
20
30
40
50
60
70
80
cilium assembly
cell projection organization
cilium movement
flagellated sperm motility
intraciliary transport
epithelial cilium movement…
non-motile cilium assembly
determination of left/right symmetry
axoneme assembly
motile cilium assembly

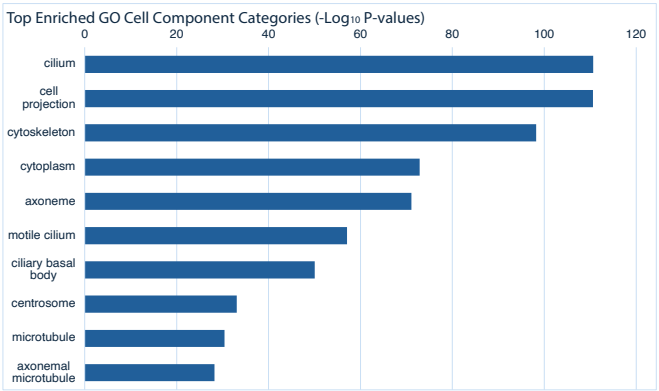
Top Enriched GO Cell Component Categories (-Log10 P-values)
0
20
40
60
80
100
120
cilium
cell projection
cytoskeleton
cytoplasm
axoneme
motile cilium
ciliary basal body
centrosome
microtubule
axonemal microtubule

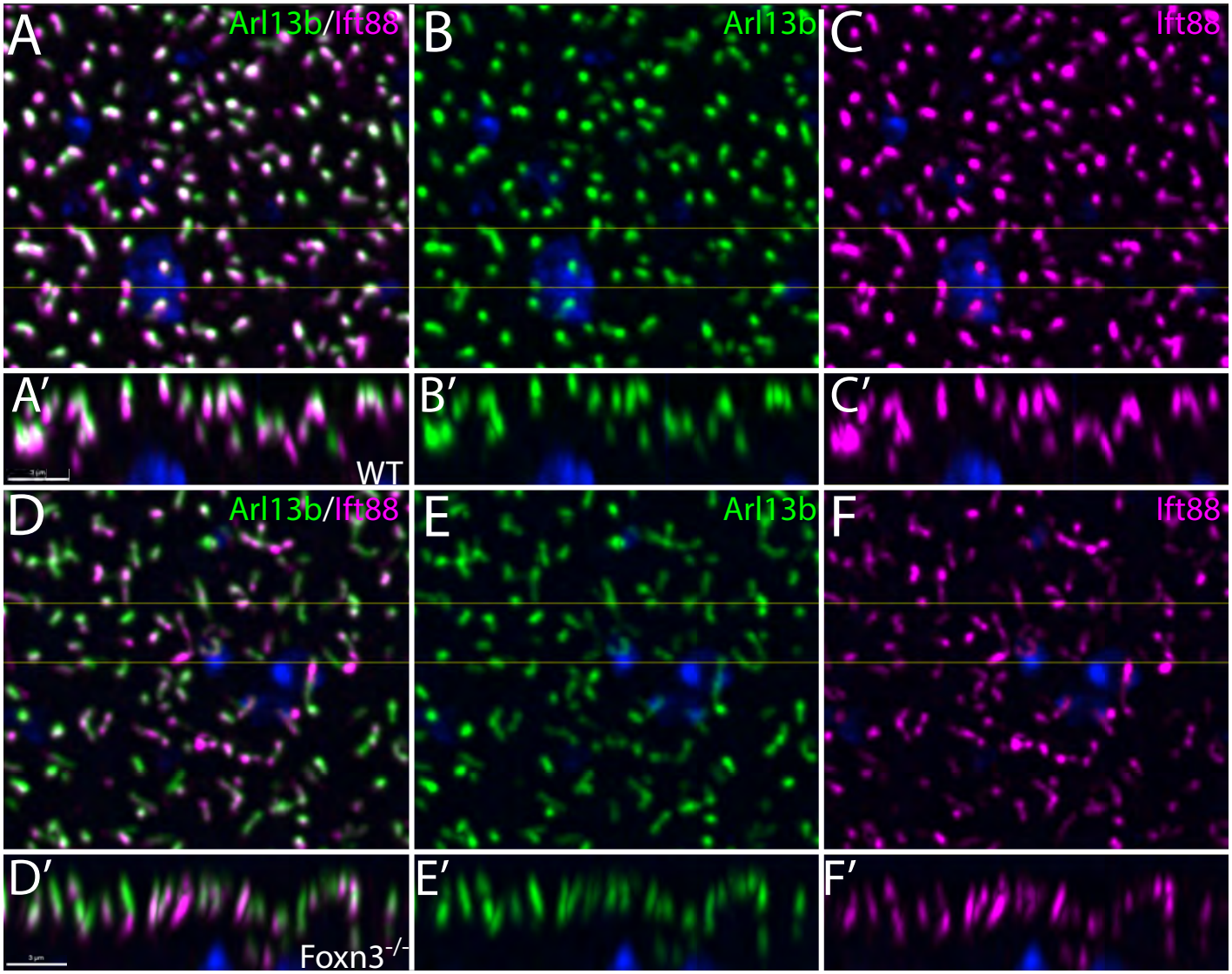
A
Arl13b/Ift88
B
Arl13b
C
Ift88
A′
B′
C′
WT
D
Arl13b/Ift88
E
Arl13b
F
Ift88
D′
E′
F′
Foxn3-/-

A

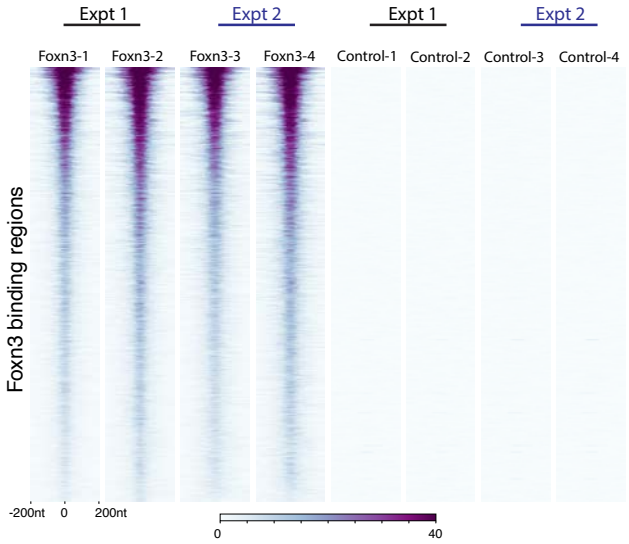

B

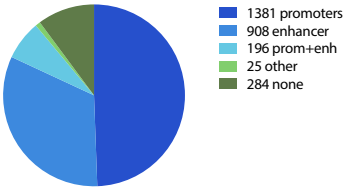

C

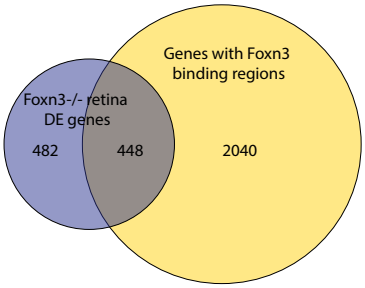

D

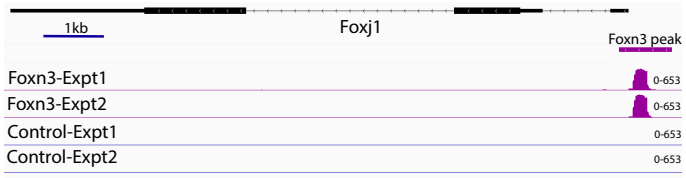

E

Motif	Name	P-val	Foxn3 Peaks
	FHL-N	1e-66	48.39%
	FHL	1e-60	78.17%
	FKH	1e-4	8.48%
	Rfx-like (de novo)	1e-703	44.49%
	Rfx3	1e-548	24.73%
	Rfx7	1e-245	60.42%

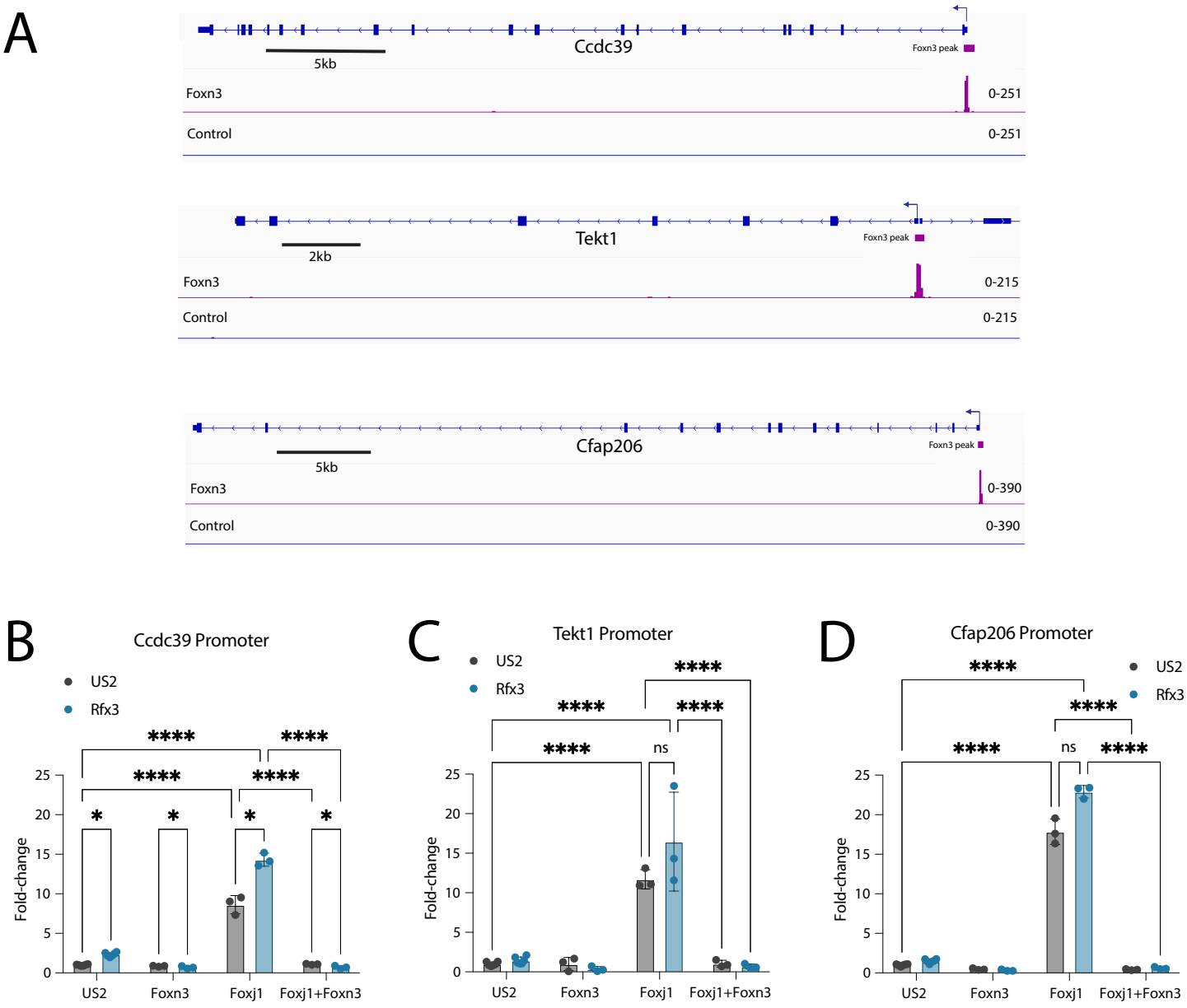
A
Ccdc39
5kb
Foxn3 peak
Foxn3
0-251
Control
0-251
Tekt1
2kb
Foxn3 peak
Foxn3
0-215
Control
0-215
Cfap206
5kb
Foxn3 peak
Foxn3
0-390
Control
0-390
B
Ccdc39 Promoter
US2
Rfx3
Fold-change
US2
Foxn3
Foxj1
Foxj1+Foxn3
C
Tekt1 Promoter
US2
Rfx3
Fold-change
ns
D
Cfap206 Promoter
US2
Rfx3
Fold-change
ns

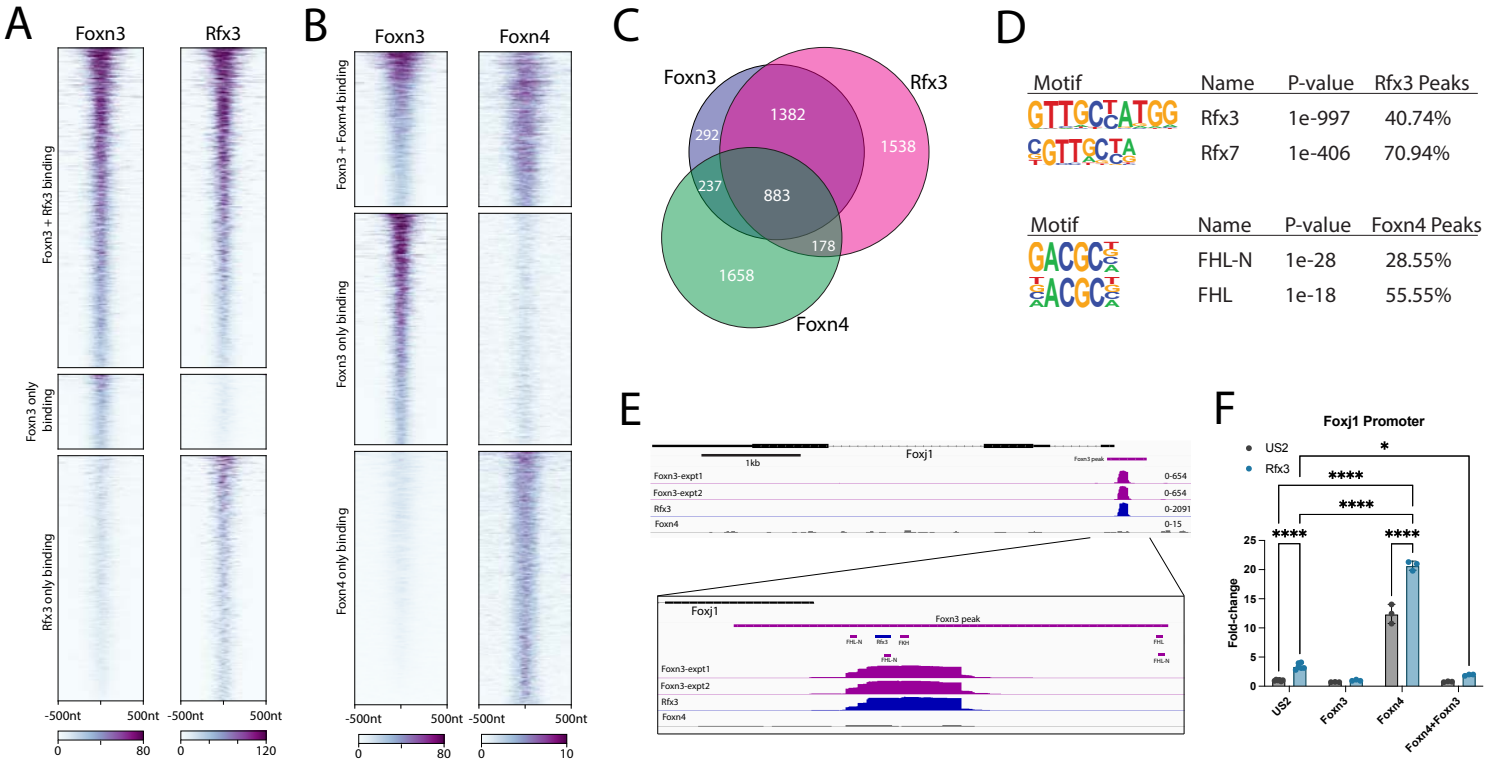
A
Foxn3
Rfx3
Foxn3 + Rfx3 binding
Foxn3 only binding
Rfx3 only binding
-500nt
500nt
0
80
120
B
Foxn3
Foxn4
Foxn3 + Foxn4 binding
Foxn3 only binding
Foxn4 only binding
10
C
Foxn3
Rfx3
Foxn4
1382
292
1538
237
883
178
1658
D
Motif
Name
P-value
Rfx3 Peaks
Rfx3
1e-997
40.74%
Rfx7
1e-406
70.94%
Motif
Name
P-value
Foxn4 Peaks
FHL-N
1e-28
28.55%
FHL
1e-18
55.55%
E
Foxj1
1kb
Foxn3-expt1
Foxn3-expt2
Rfx3
Foxn4
Foxn3 peak
F
Foxj1 Promoter
US2
Rfx3
Fold-change
Foxn3
Foxn4
Foxn4+Foxn3

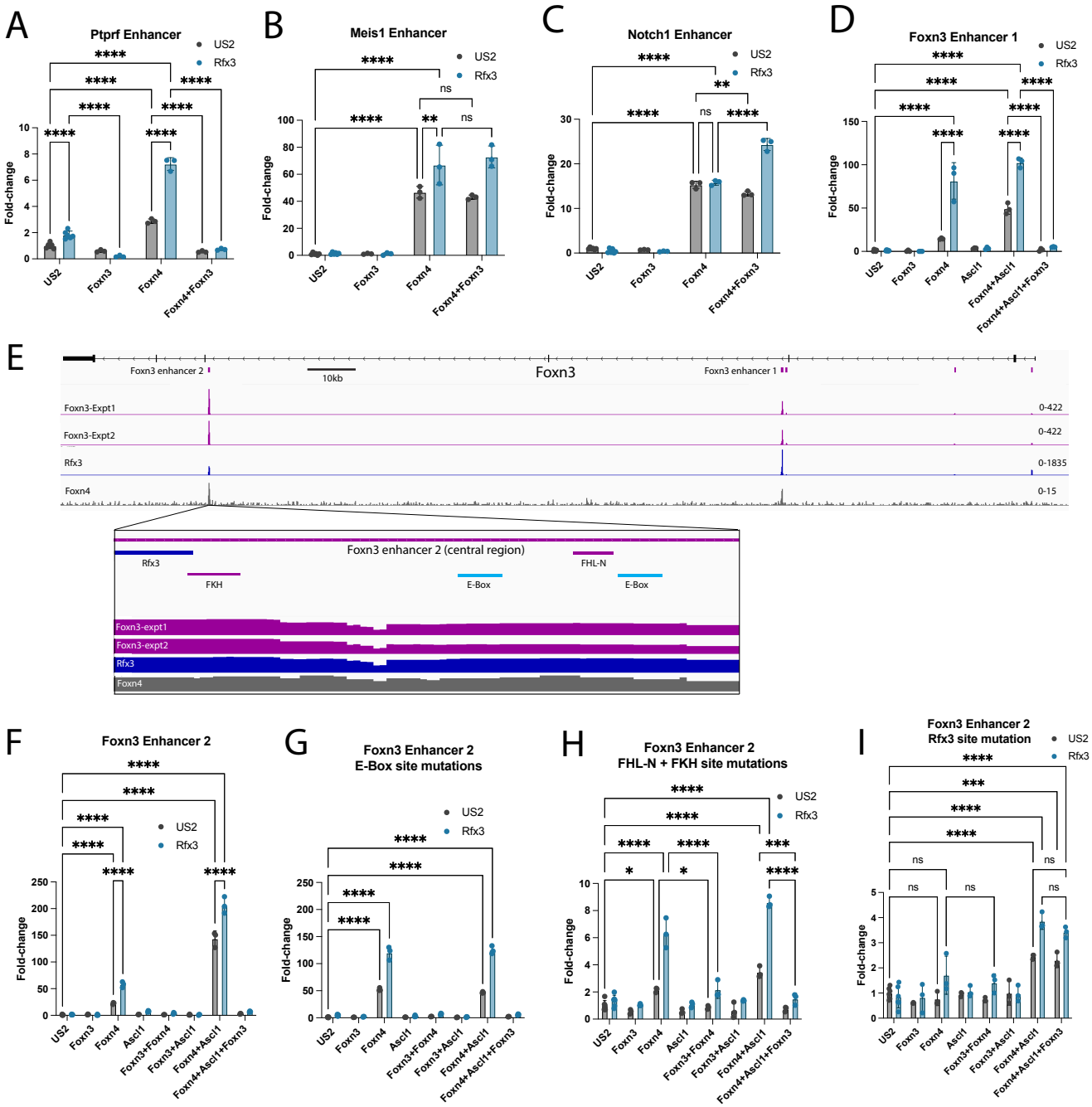
A
Ptprf Enhancer
US2
Rfx3
Fold-change
US2
Foxn3
Foxn4
Foxn4+Foxn3
B
Meis1 Enhancer
C
Notch1 Enhancer
D
Foxn3 Enhancer 1
Ascl1
Foxn4+Ascl1
Foxn4+Ascl1+Foxn3
E
Foxn3 enhancer 2
10kb
Foxn3
Foxn3 enhancer 1
Foxn3-Expt1
Foxn3-Expt2
Rfx3
Foxn4
0-422
0-1835
0-15
Foxn3 enhancer 2 (central region)
FHL-N
FKH
E-Box
F
Foxn3 Enhancer 2
Foxn3+Foxn4
Foxn3+Ascl1
Foxn4+Ascl1
Foxn4+Ascl1+Foxn3
G
Foxn3 Enhancer 2
E-Box site mutations
H
Foxn3 Enhancer 2
FHL-N + FKH site mutations
I
Foxn3 Enhancer 2
Rfx3 site mutation

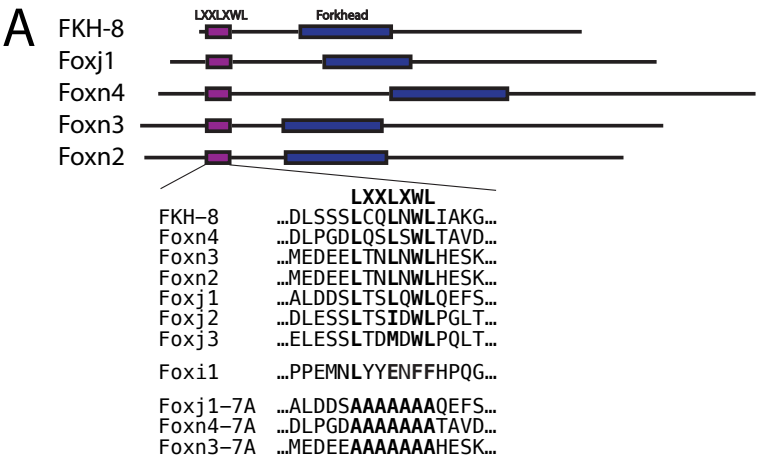
A
FKH-8
Foxj1
Foxn4
Foxn3
Foxn2
LXXLXWL
Forkhead
LXXLXWL
FKH-8 …DLSSSLCQLNWLIAKG…
Foxn4 …DLPGDLQSLSWLTAVD…
Foxn3 …MEDEELTNLNWLHESK…
Foxn2 …MEDEELTNLNWLHESK…
Foxj1 …ALDDSLTSLQWLQEFS…
Foxj2 …DLESSLTSIDWLPGLT…
Foxj3 …ELESSLTDMDWLPQLT…
Foxi1 …PPEMNLYYENFFHPQG…
Foxj1-7A …ALDDSAAAAAAAQEFS…
Foxn4-7A …DLPGDAAAAAAATAVD…
Foxn3-7A …MEDEEAAAAAAAHESK…

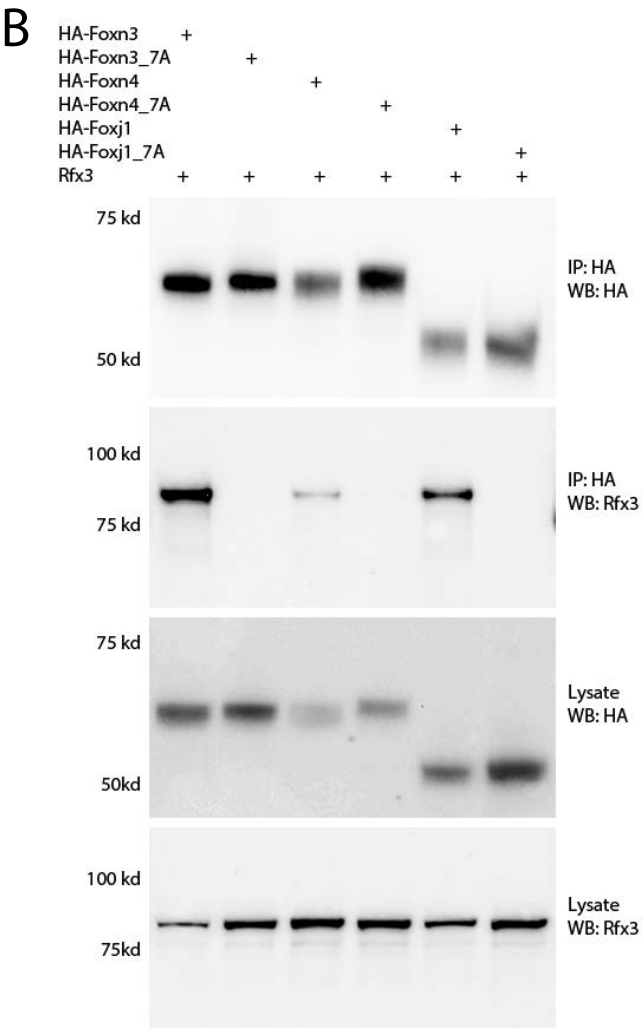
B
HA-Foxn3
HA-Foxn3_7A
HA-Foxn4
HA-Foxn4_7A
HA-Foxj1
HA-Foxj1_7A
Rfx3
75 kd
50 kd
IP: HA
WB: HA
100 kd
75 kd
IP: HA
WB: Rfx3
75 kd
50kd
Lysate
WB: HA
100 kd
75kd
Lysate
WB: Rfx3

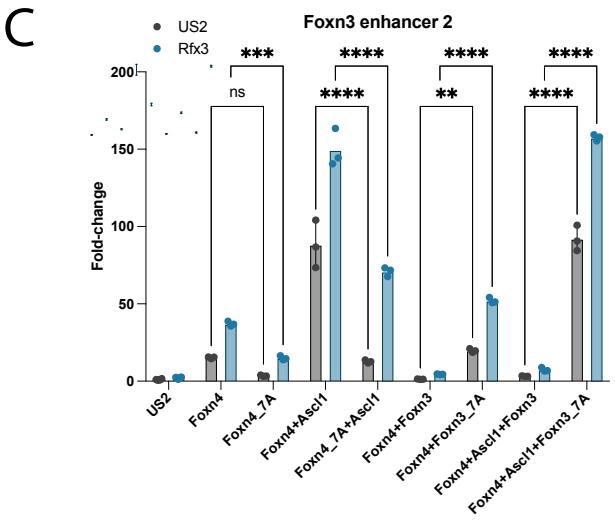
C
Foxn3 enhancer 2
US2
Rfx3
Fold-change
200
150
100
50
0
ns
***
****
**
US2
Foxn4
Foxn4_7A
Foxn4+Ascl1
Foxn4_7A+Ascl1
Foxn4+Foxn3
Foxn4+Foxn3_7A
Foxn4+Ascl1+Foxn3
Foxn4+Ascl1+Foxn3_7A